

1 **Evaluation of high-resolution gridded climate products in reproducing spatial and**  
2 **temporal variation in precipitation in central Panama**

3

4 Vicente Vasquez<sup>1,2\*</sup> and Helene C. Muller-Landau<sup>1</sup>

5

6 <sup>1</sup> Smithsonian Tropical Research Institute, P.O. Box 0843-03092, Balboa Ancón, Republic of  
7 Panamá

8 <sup>2</sup> School of Forest, Fisheries and Geomatics Science, University of Florida, 349 Newins-Ziegler  
9 Hall, Gainesville, Florida, 32611, USA

10

11 \* Corresponding author: [vasquezvicente@ufl.edu](mailto:vasquezvicente@ufl.edu), [vasquezv@si.com](mailto:vasquezv@si.com), vicenteavv7@gmail.com

12

13 Revised manuscript submitted for consideration for publication in the planned volume, *The First*  
14 *100 Years of Research on Barro Colorado: The Physical Basis*, ed. R. F. Stallard. Washington,  
15 DC: Smithsonian Institution Scholarly Press.

16 **Abstract**

17 Tropical forests vary widely in their precipitation regimes and seasonal water availability, but  
18 high-quality in-situ (ground-based) meteorological data are rare, and few studies have evaluated  
19 the performance of global gridded climate products in the tropics. We compared the performance  
20 of eleven high-resolution gridded climate products against in-situ datasets spanning high rainfall  
21 variation in central Panama. The gridded products differed widely in their performance, although  
22 most captured the broad trends of spatial and seasonal rainfall variation in central Panama, and  
23 all underestimated precipitation in the wettest sites, especially in the dry season. Spatial, seasonal  
24 and interannual variation were best captured by CHIRPSv2; downscaled finer-resolution  
25 products performed similarly well in reproducing spatial variation. Our ability to quantify  
26 performance was constrained by limited data availability, even in this region with relatively  
27 many in-situ datasets, highlighting the need for more investment in ground-based data collection  
28 in the tropics.

29

30 **Keywords:** precipitation, Panama, climate reanalysis, satellite-based precipitation; rain gauge;  
31 validation; tropical forests

32

### 33 **Introduction**

34 Tropical forests vary widely in their total annual precipitation and its seasonal  
35 distribution, and thus in the frequency, intensity and duration of drought stress, and this in turn  
36 drives considerable variation in tropical forest communities and ecosystems (Muller-Landau et  
37 al., 2021). Information on local climate, and especially precipitation, is thus critically important  
38 for ecological studies in tropical forests. Research on Barro Colorado Island (BCI) has benefited  
39 from an exceptionally strong meteorological monitoring program (Paton and Stallard, 2023).  
40 However, such high-quality in-situ (ground-based) meteorological data are relatively scarce in  
41 Panama and most other tropical forest regions (Malhi and Wright, 2004; Clark, 2007).

42 Global gridded climate products provide a potential alternative for characterizing climate  
43 when local measurements are not available (Burton et al., 2018). These global climate products  
44 are produced by combining data from in-situ and/or satellite sensors with statistical and/or  
45 mechanistic models. A plethora of such datasets now yields a wide array of options for  
46 researchers, e.g., an initial search for this study yielded 23 publicly available precipitation  
47 products (Table S1). Unfortunately, relatively few studies have evaluated the performance of any  
48 of these datasets in reproducing spatial and temporal climate variation in tropical landscapes,  
49 much less provided quantitative comparisons to inform choice among these datasets (Trenberth  
50 et al., 2001; Burton et al., 2018).

51 Central Panama is an excellent region for evaluating the performance of global climate  
52 products in reproducing precipitation patterns in the tropics. Annual precipitation varies more  
53 than twofold due to a steep rainfall gradient from the drier Pacific to the wetter Caribbean side of  
54 the isthmus, as well as elevational rainfall variation (Muller-Landau et al., 2024; Paton and  
55 Stallard, in preparation). The region hosts a relatively large number of high-quality, long-term

56 rainfall monitoring sites, reflecting the importance of rainfall for the operation of the Panama  
57 Canal and for the scientific mission of the Smithsonian Tropical Research Institute (Paton, 2022;  
58 Paton, 2023; Paton and Stallard, 2023; Wright and Muller-Landau, 2024).

59 Here, we evaluate eleven high-spatial-resolution gridded climate datasets against in-situ  
60 rainfall data in central Panama. We (1) assess their ability to capture spatial variation including  
61 the steep regional rainfall gradient, and (2) evaluate their accuracy and precision in reproducing  
62 seasonal and interannual variation. Our aim is to provide guidance for researchers seeking to  
63 choose among available gridded datasets to estimate rainfall in tropical sites lacking nearby  
64 ground stations. We treated the in-situ data as “truth” in evaluating the gridded climate datasets,  
65 though we recognize that not all differences reflect errors in the global gridded climate products.  
66 Most fundamentally, rain gauge data capture rainfall at a single point ( $<0.1 \text{ m}^2$ ) in a region with  
67 high local stochastic rainfall variation, whereas gridded climate products provide values for  
68 average rainfall over an area more than a million times larger ( $>1 \text{ km}^2$ ). Rain gauges can also  
69 systematically underestimate precipitation by  $\sim 9\text{-}23\%$  due to wind effects and evaporation  
70 (Pollock et al., 2018).

71

## 72 **Methods**

### 73 *Study region*

74 Our study region is located in Central Panama, extending from  $8.8^\circ$  to  $9.5^\circ$  N latitude and  
75 from  $80.2^\circ$  to  $79.4^\circ$  W longitude. This region includes the Panama Canal and Barro Colorado  
76 Island (Figure 1). It encompasses a narrow isthmus with a steep regional rainfall gradient from

77 the drier Pacific to the wetter Caribbean side, as well as a 425 km<sup>2</sup> artificial lake (Gatun Lake,  
78 since 1913) and orographic variation from sea level to 1340 m elevation.

79         Rainfall is seasonally variable in this region, with a dry season extending on average  
80 from late December to late April. The length and severity of the dry season vary among sites and  
81 plays a major role in determining tree species composition (Condit et al. 2013) and patterns of  
82 deciduousness (Bohlman 2010).

### 83 *Datasets*

84         We evaluated gridded climate datasets against in-situ rainfall data for 31 stations,  
85 including 29 maintained by the Panama Canal Authority (ACP) and 2 maintained by the  
86 Smithsonian Tropical Research Institute (STRI). Rainfall data were collected using electronic  
87 tipping buckets for ACP data, and both manual and electronic sensors for STRI data, with some  
88 changes in sensor models over time (Paton, 2022). The selected ground stations had relatively  
89 complete data during the years covered by the gridded datasets and were a subset of 100 ground  
90 stations that were initially considered for inclusion (Table S2). Analyses of temporal variation  
91 were further restricted to just nine stations with the longest time records, as detailed below.

92         We evaluated precipitation products from 11 publicly available gridded climate datasets  
93 with spatial resolutions of 0.05 degrees (approximately 5.5 km) or finer (Table 1, see also Table  
94 S1 for a complete list of datasets considered). We did not consider coarser resolution products  
95 because of the steepness of climate gradients in the focal region. The temporal coverage varied  
96 among gridded datasets and spanned 1970-2016. The gridded climate products evaluated here  
97 are not independent – they share many of the same forcing datasets and/or algorithms (Table 1).  
98 For comparisons with ground stations, we extracted raster cell values at each station's

99 coordinates using a nearest-neighbor approach (implemented with the terra package, Hijmans et  
100 al., 2023). If this returned a null value (e.g., for stations located in grid cells dominated by  
101 water), we instead used the nearest non-null cell. Some stations are spatially close to each other  
102 and therefore fall within the same raster cell for some or all gridded datasets (Table S3). For  
103 visualization purposes, gridded datasets were resampled using nearest-neighbor at 0.008333-  
104 degree resolution (terra package, Hijmans et al., 2023).

105

### 106 *Analyses of spatial variation*

107 Our spatial variation analyses focused on two response variables: total annual  
108 precipitation and total January to April precipitation, the latter a proxy for dry season  
109 precipitation. We chose to evaluate dry season precipitation in addition to annual precipitation  
110 because dry season precipitation is especially important for the biota and ecosystem function. We  
111 also ran analyses of wet season precipitation initially, but those results paralleled those for  
112 annual precipitation, and thus we do not include them here. To visualize spatial patterns of  
113 precipitation for each gridded dataset, we computed average annual precipitation and average  
114 January to April precipitation for each grid cell of each dataset and mapped these across the  
115 region.

116 We evaluated the ability of the gridded datasets to reproduce spatial variation using in-  
117 situ data for 31 stations each having 30 or more years of data during 1970-2016 (Figure 1). The  
118 comparisons with gridded datasets were based on the means for each ground station over the  
119 relevant span of years (which varied among gridded datasets). In computing site-specific means,  
120 in-situ data were used as reported for site-year combinations with complete records (annual

121 precipitation required data for all 12 months, and dry-season precipitation required data for all  
122 four months from January to April). We gap-filled the remainder of the ground station time  
123 series of annual precipitation and January to April precipitation before computing means for each  
124 ground station. Specifically, for each response variable (annual precipitation, January to April  
125 precipitation), we fit linear mixed models with fixed effects for site ( $s$ ) and random effects for  
126 year ( $t$ ), using data from the entire historical record, and only including site-year combinations  
127 with 12 months for the annual precipitation model and the 4 dry season months for the January to  
128 April precipitation model. For example, for annual precipitation,  $P$ , we fit:

$$129 \quad P_{st} = \beta_s + c_t + \epsilon_i$$

130 Where  $P_{st}$  is the annual precipitation in site  $s$  in year  $t$ ,  $\beta_s$  is the fixed effect for site,  $c_t$  is the  
131 random effect of year (normally distributed with mean 0 and fitted variance  $\sigma_{year}^2$ ) and  $\epsilon_i$  is the  
132 residual error term. We then predicted  $P_{st}$  in year-site combinations without data from the fitted  
133  $\beta_s$  and  $c_t$ . In total, 136 out of 1457 values of mean annual precipitation for ground sites were gap-  
134 filled in the 1970-2016 timeseries for the 31 sites. The proportion of gap-filled data varied  
135 among gridded datasets, depending on the temporal extent of the gridded dataset and the  
136 availability of station observations within that period (Figure S2).

137 We visualized and quantified the performance of each gridded dataset in capturing spatial  
138 variation in each response variable using scatterplots, linear regressions (for predicting the in-situ  
139 data from the gridded data), and the following metrics: the Pearson correlation coefficient ( $r$ ),  
140 root mean square error (RMSE), mean absolute error (MAE) and mean bias across the 31  
141 stations. These metrics were calculated as:

142 
$$r = \frac{\sum(x_i - \bar{x})(y_i - \bar{y})}{\sqrt{\sum(x_i - \bar{x})^2 \sum(y_i - \bar{y})^2}}$$

143 
$$RMSE = \sqrt{\sum_{i=1}^n \frac{(y_i - x_i)^2}{n}}$$

144 
$$MAE = \frac{1}{n} \sum |y_i - x_i|$$

145 
$$Mean\ bias = \frac{1}{n} \sum (y_i - x_i)$$

146 where  $y_i$  is the value for the gridded dataset for site  $i$ ,  $x_i$  is in-situ value for site  $i$ , and  $n$  is the  
147 number of sites.

148 *Analyses of temporal variation*

149 We evaluated the performance of the gridded datasets in capturing seasonal variation and  
150 interannual variation in precipitation at nine focal ground stations that each had 44 or more years  
151 of data during 1970-2016. Mean total annual rainfall during 1970-2016 ranged from 2088 to  
152 3947 mm/year among the focal stations. For interannual and seasonal temporal variation  
153 analyses, missing values in the ground data were not gap-filled but simply omitted.

154

155 The temporal variation analyses included two precipitation records for Barro Colorado  
156 Island which fall within the same grid cell. The station named BCICLEAR is the STRI  
157 meteorological record from the lab clearing area, which combines data from an automated  
158 tipping bucket with a manual rain gauge (an average of two manual gauges, with missing days

159 filled by prorating the rainfall recorded at the end of the gap based on electronic sensor data).  
160 The station named BCI is the ACP electronic gauge located near the edge of Gatun Lake.

161 To evaluate performance in capturing seasonal variation, we first calculated the mean  
162 rainfall for each calendar month at each site for the year's corresponding to each gridded dataset,  
163 then calculated Pearson correlation coefficients, and RMSE over the 12 calendar months for each  
164 site and dataset and finally averaged these statistics over the ten records for each dataset.

165 To evaluate performance in capturing interannual variation, we calculated Pearson  
166 correlation coefficients and RMSE for total annual rainfall across years for each site and year  
167 and then averaged the results over datasets. Interannual variability could be assessed only for six  
168 gridded datasets with publicly available timeseries between 1979 and 2016.

169 All analyses and visualizations were conducted in R version 4.2.1 (R Core Team, 2022)  
170 using the packages terra, sp, tmap, lme4, basemaps (Hijmans et al., 2023; Pebesma and Bivand,  
171 2005; Tennekes, 2018; Bates et al., 2015; Schwalb-Willmann, 2024). Complete code is provided  
172 in the associated repository (Vasquez, 2024).

173

## 174 **Results**

### 175 *Spatial patterns*

176 All the gridded datasets correctly capture the direction of regional precipitation trends,  
177 showing higher annual precipitation at higher elevation and on the Caribbean (northwest) side of  
178 the isthmus, but they differ widely in the strength of these gradients and the details of the  
179 patterns (Figure 2, top). The datasets differ even more strongly in their spatial patterns of January

180 to April (dry season) precipitation (Figure 2, bottom). In general, the gridded datasets  
181 systematically underestimate precipitation at the wettest sites, those at high elevation and along  
182 the Caribbean coast (Figure 3). The gridded precipitation datasets perform moderately well in  
183 capturing spatial variation in mean annual precipitation, with Pearson correlation coefficients  
184 with in-situ data averaging 0.73 (range 0.35-0.88), and less well for January to April  
185 precipitation, with correlation coefficients averaging 0.61 (range 0.14-0.88) (Table 2, Figure 4).  
186 All gridded datasets exhibit substantial differences relative to ground measurements, with RMSE  
187 of 276-548 mm for annual precipitation, and 80-130 mm for dry season precipitation. The  
188 spatial pattern for total annual precipitation across the in-situ stations is best captured by  
189 CHIRPS v2.0, CHELSA 2.1, CHELSA EarthEnv, and CHPclim v1.0, while CHIRPS v2.0,  
190 TerraClimate and CHPclim v1.0 best capture the variation in Jan-Apr precipitation (Pearson  
191  $r > 0.8$  in all cases). The CHIRPS v2.0 dataset had the lowest RMSE and MAE for both total  
192 annual precipitation and January-to-April precipitation.

193         The datasets vary strongly in their biases relative to the in-situ data. Given the known  
194 tendency towards under-catchment in rain gauge measurements, we expected all the gridded  
195 datasets to exhibit substantial positive biases relative to the in-situ data. For total annual  
196 precipitation, 7 of 11 gridded datasets average substantially higher values consistent with this  
197 expectation, but the remaining 4 showed small negative bias (mean bias ranged from -44 to +418  
198 mm; Table 2, Figure 3). Further, 10 of 11 gridded datasets systematically underestimate dry  
199 season precipitation relative to in-situ data (mean bias ranged from -63 to +5 mm, Table 2,  
200 Figure 3). Inspection of the bias patterns across sites reveals that the gridded products all exhibit  
201 the expected modest positive bias (higher values than in-situ) in the lower rainfall lowland sites,  
202 and all have strong negative bias at high rainfall high elevation sites (Figures 3 and 4). The

203 PBCOR-corrected datasets have higher precipitation totals, and thus systematically shift the  
204 mean bias upwards.

205

## 206 *Seasonal and interannual patterns*

207 All gridded datasets did well at reproducing the broad patterns of seasonal variation in  
208 mean rainfall among calendar months (Pearson correlations between 0.93 and 0.98, Table 2).  
209 However, all underestimated dry season precipitation at the wettest sites (Figure 5). CHIRPS  
210 v2.0 had the highest Pearson correlation for seasonality (0.98) and the smallest average RMSE  
211 (23 mm).

212 Interannual variability in annual precipitation was less well reproduced in the gridded  
213 climate products, especially at the wetter sites (Figure 6). The best datasets – specifically  
214 CHIRPS v2.0 and CHELSA W5E5 – had mean Pearson correlation coefficients of 0.74 and 0.69,  
215 respectively, and other datasets did much worse ( $r=0.26$  to  $0.59$ , Table 2).

216

## 217 **Discussion**

### 218 *Performance of gridded precipitation products*

219 The high-resolution gridded precipitation products analyzed here all did moderately well  
220 in capturing the broad trends of spatial and seasonal variation in precipitation in central Panama,  
221 as reflected in high Pearson correlations. However, all of them underestimated precipitation in  
222 the wettest sites, especially dry season precipitation. In general, the products performed less well

223 at reproducing spatial variation in dry season precipitation than in total annual precipitation, and  
224 less well at reproducing interannual variation than seasonal variation.

225 Our results provide a basis for specific recommendations on which products are best for  
226 various applications, at least for the study region. For analyses requiring time series, we  
227 recommend CHIRPS v2.0, whose monthly product best captured seasonal and interannual  
228 variation, and which is available at daily resolution from 1981 to near real time. CHIRPS v2.0  
229 also performed well in reproducing spatial variation among ground stations in our study region,  
230 even though it has only 0.05 degree (~5 km) spatial resolution, and thus it is also our top  
231 recommendation for studies of among-site variation in central Panama. For studies requiring  
232 finer spatial resolution, the best 1-km resolution dataset we evaluated was CHELSA 2.1,  
233 although it did much more poorly than CHIRPS v2.0 at capturing spatial variation in dry season  
234 precipitation among our 31 focal ground stations. We expect that downscaling of the CHIRPS  
235 product would likely perform even better (e.g., Retalis et al., 2017). We note that WorldClim  
236 datasets performed particularly poorly, and we advise against their use.

237 The steep precipitation gradient of Panama, the narrow isthmus, and high topographic  
238 heterogeneity creates high local variability in precipitation, which is inherently missed by coarser  
239 resolution products. We thus included only products with at least 0.05 degrees resolution in our  
240 evaluation. In other tropical regions without such fine-scale spatial heterogeneity, coarser  
241 resolution products such as IMERG(GPM) may perform equally well and should be considered.

242

243 *Interpretation and comparisons with other studies*

244 Interpretation of differences among the climate products in RMSE, MAE and mean bias  
245 relative to the in-situ data is complicated by the known systematic undercatch in rain gauge  
246 measurements, as well as by the fact that some of our in-situ datasets also directly contribute to  
247 some of the gridded climate products. Given that in-situ data can systematically underestimate  
248 rainfall, accurate climate products should show substantial positive mean bias relative to the in-  
249 situ observations, and this will elevate their RMSE and MAE in our analyses. Most of the  
250 climate products showed substantial positive mean bias (90-414mm) for total annual  
251 precipitation, on the order of what would be expected to compensate for undercatch. The  
252 exceptions are WorldClim and TERRA, which share a forcing dataset that is an observational  
253 network, thus approximating closer in-situ values. Some of our in-situ stations are included in the  
254 observational datasets that inform WorldClim, TERRA, and CHPclim v1.0, and thus we expect  
255 these products to exhibit higher performance relative to these in-situ datasets, even though they  
256 are likely to perform more poorly at independent validation stations. It's important to keep in  
257 mind that the gridded climate products evaluated here are not all independent – there are many  
258 shared forcing datasets among them, which can in part explain similarities in performance (Table  
259 1).

260 Our findings on the performance of gridded precipitation products are broadly consistent  
261 with previous studies, although there have been few studies in the tropics, and most of those have  
262 included only one or a few gridded products. López-Bermeo et al. (2022) and Paredes Trejo et al.  
263 (2016) found that CHIRPSv2 does well in reproducing spatial, seasonal, and interannual  
264 variation in rainfall in the Antioquia region of Colombia and in Venezuela, respectively. Burton  
265 et al (2018) evaluated CHIRPS and three other satellite-based rainfall products in tropical South  
266 America and Africa, finding that CHIRPS and TRMM did best (we did not include TRMM in

267 our analysis because of its coarse resolution of 0.25 degrees). Bastidas Oejo et al. (2019) found  
268 that CHELSA1.2 and Worldclim both showed very good performance in reproducing rainfall  
269 patterns in northwest Colombia, with CHELSA1.2 doing better, also consistent with our  
270 findings.

271

### 272 *Recommendations for future research*

273 Future analyses should build on the work here by incorporating additional in-situ  
274 datasets, applying more sophisticated methods to assess the performance of the gridded climate  
275 products, and evaluating additional variables. We included only rain gauges in our evaluation;  
276 data from local weather radar, weirs, and measurements of river and lake levels could be  
277 integrated to more comprehensively assess precipitation patterns. Their inclusion would require  
278 more complex analyses, including accounting for distance effects in the radar data and applying  
279 hydrological models to link rainfall with runoff. The rain gauge data could also be better utilized  
280 by incorporating explicit, empirically supported models for how point measurements such as rain  
281 gauges are expected to differ from average values over large areas, ideally also accounting for  
282 environmental heterogeneity within grid cells, and by incorporating sites with shorter time series.  
283 Furthermore, additional research is necessary to evaluate the electronic sensors' tendency to  
284 underestimate rainfall, considering the variability in sensor types utilized at each station and the  
285 potential impacts of climate and surrounding vegetation on point measurements. Here we  
286 evaluated only precipitation; a more complete treatment would also encompass other variables  
287 important for predicting drought stress and forest ecosystem function, notably including potential  
288 evapotranspiration, solar radiation, temperature, and windspeed.

289 Our ability to quantify performance was constrained by limited data availability, even in  
290 this region with relatively many high-quality, long-term in-situ datasets. For example, the  
291 gridded datasets exhibit quite different patterns of precipitation in the northwestern area  
292 examined, which lacked ground stations for evaluation (Figures 1 and 2). The relatively good  
293 performance of the gridded products should not be taken as a reason to reduce investment in  
294 ground data. These products ultimately depend on high-quality in-situ data, which are  
295 incorporated into these products in multiple ways. Especially given the high topographic and  
296 land cover heterogeneity in this region, a denser and more evenly placed network of stations is  
297 needed to fully capture regional climate variation, better evaluate the gridded products, and  
298 contribute to better products themselves. We thus recommend investing more in meteorological  
299 data collection and curation.

300

### 301 **Acknowledgments**

302 We gratefully acknowledge the work of Steven Paton and many technicians at the STRI's long-  
303 term meteorological monitoring program and the Autoridad del Canal de Panama (as well as its  
304 precursor, the Panama Canal Commission) in collecting, cleaning, and curating the in-situ  
305 meteorological data. This work builds on previous unpublished analyses and code by KC  
306 Cushman.

307

### 308 **References**

309 Abatzoglou, J. T., S. Z. Dobrowski, S. A. Parks, and K. C. Hegewisch. 2018. TerraClimate, a  
310 high-resolution global dataset of monthly climate and climatic water balance from 1958–  
311 2015. *Scientific Data*, 5: 170191. <https://doi.org/10.1038/sdata.2017.191>

312 Bastidas Osejo, B., T. B. Vargas, and J. A. Martinez. 2019. Spatial distribution of precipitation  
313 and evapotranspiration estimates from WorldClim and Chelsa datasets: Improving long-  
314 term water balance at the watershed-scale in the Urabá region of Colombia. *International*  
315 *Journal of Sustainable Development and Planning*, 14: 105-117.  
316 <https://doi.org/10.2495/SDP-V14-N2-105-117>

317 Bates, D., Mächler, M., Bolker, B., & Walker, S. 2015) Fitting Linear Mixed-Effects Models  
318 Using **lme4**. *Journal of Statistical Software*, 67(1). <https://doi.org/10.18637/jss.v067.i01>

319 Beck, H. E., T. R. McVicar, M. Zambrano-Bigiarini, C. Alvarez-Garret, O. M. Baez-Villanueva,  
320 J. Sheffield, D. Karger, and E. F. Wood. 2020. Bias correction of global high-resolution  
321 precipitation climatologies using streamflow observations from 9372 catchments. *Journal*  
322 *of Climate*, 33: 1299-1315. <https://doi.org/10.1175/JCLI-D-19-0332.1>

323 Bohlman, S. A. 2010. Landscape patterns and environmental controls of deciduousness in forests  
324 of central Panama. *Global Ecology And Biogeography*, 19: 376-385.  
325 <https://doi.org/10.1111/j.1466-8238.2009.00518.x>

326

327 Burton, C., S. Rifai, and Y. Malhi. 2018. Inter-comparison and assessment of gridded climate  
328 products over tropical forests during the 2015/2016 El Niño. *Philosophical Transactions*  
329 *of the Royal Society B: Biological Sciences*, 373. <https://doi.org/10.1098/rstb.2017.0406>

330 Clark, D. A. 2007. Detecting tropical forests' responses to global climatic and atmospheric  
331 change: current challenges and a way forward. *Biotropica*, 39: 4-19.

332 Condit, R., B. M. J. Engelbrecht, D. Pino, R. Perez, and B. L. Turner. 2013. Species distributions  
333 in response to individual soil nutrients and seasonal drought across a community of  
334 tropical trees. *Proceedings Of The National Academy Of Sciences Of The United States  
335 Of America*, 110: 5064-5068. <https://doi.org/10.1073/pnas.1218042110>

336 Fick, S. E., and R. J. Hijmans. 2017. WorldClim 2: new 1-km spatial resolution climate surfaces  
337 for global land areas. *International Journal of Climatology*, 37: 4302-4315.  
338 <https://doi.org/10.1002/joc.5086>

339 Funk, C., A. Verdin, J. Michaelsen, P. Peterson, D. Pedreros, and G. Husak. 2015. A global  
340 satellite-assisted precipitation climatology. *Earth Syst. Sci. Data*, 7: 275-287.  
341 <https://doi.org/10.5194/essd-7-275-2015>Funk, C., Peterson, P., Landsfeld, M., Pedreros,  
342 D., Verdin, J., Shukla, S., Husak, G., Rowland, J., Harrison, L., Hoell, A., & Michaelsen,  
343 J. 2015. The climate hazards infrared precipitation with stations—a new environmental  
344 record for monitoring extremes. *Scientific Data*, 2(1), 150066.  
345 <https://doi.org/10.1038/sdata.2015.66>

346 Hijmans, R., R. Bivand, E. Pebesma, and M. Summer. 2023a. terra: Spatial Data Analysis (1.7-3)  
347 [R package].

348 Karger, D. N., O. Conrad, J. Böhner, T. Kawohl, H. Kreft, R. W. Soria-Auza, N. E.  
349 Zimmermann, H. P. Linder, and M. Kessler. 2018. Data from: Climatologies at high  
350 resolution for the earth’s land surface areas. *EnviDat*.  
351 <https://doi.org/https://doi.org/10.16904/envidat.228.v2.1>

352 Karger, D. N., S. Lange, C. Hari, C. P. O. Reyer, and N. E. Zimmermann. 2021a. CHELSA-  
353 W5E5 v1.1: W5E5 v1.0 downscaled with CHELSA v2.0. ISIMIP Repository.  
354 <https://doi.org/10.48364/ISIMIP.836809.1>

355 Karger, D. N., A. M. Wilson, C. Mahony, N. E. Zimmermann, and W. Jetz. 2021b. Global daily  
356 1km land surface precipitation based on cloud cover-informed downscaling. *Scientific*  
357 *Data*. <https://doi.org/doi.org/10.1038/s41597-021-01084-6>

358 López-Bermeo, C., R. D. Montoya, F. J. Caro-Lopera, and J. A. Díaz-García. 2022. Validation of  
359 the accuracy of the CHIRPS precipitation dataset at representing climate variability in a  
360 tropical mountainous region of South America. *Physics and Chemistry of the Earth, Parts*  
361 *A/B/C*, 127: 103184. <https://doi.org/10.1016/j.pce.2022.103184>

362 Malhi, Y., and J. Wright. 2004. Spatial patterns and recent trends in the climate of tropical  
363 rainforest regions. *Philosophical Transactions Of The Royal Society Of London Series B-*  
364 *Biological Sciences*, 359: 311-329. <https://doi.org/10.1098/rstb.2003.1433>

365 Muller-Landau, H. C., K. C. Cushman, E. E. Arroyo, I. Martinez Cano, K. J. Anderson-Teixeira,  
366 and B. Backiel. 2021. Patterns and mechanisms of spatial variation in tropical forest  
367 productivity, woody residence time, and biomass. *New Phytologist*, 229: 3065-3087.  
368 <https://doi.org/https://doi.org/10.1111/nph.17084>

369 Mello, S. Aguilar, S. Lao, D. Mitre, and R. Condit. 2024. Forest Biomass Carbon Stocks  
370 and Fluxes in a Broader Context: Insights and Opportunities Associated with the Central  
371 Panama Plot Network. In *The First 100 Years of Research on Barro Colorado: Plant and*  
372 *Ecosystem Science*, ed. H. C. Muller-Landau and S. J. Wright, pp. 487-498. Washington,  
373 DC: Smithsonian Institution Scholarly Press. <https://doi.org/10.5479/si.26880790>

374 Paredes Trejo, F. J., H. A. Barbosa, M. A. Peñaloza-Murillo, M. Alejandra Moreno, and A.  
375 Farías. 2016. Intercomparison of improved satellite rainfall estimation with CHIRPS  
376 gridded product and rain gauge data over Venezuela. *Atmósfera*, 29: 323-342.  
377 <https://doi.org/10.20937/ATM.2016.29.04.04>

378 Paton, S. 2022. Panama Canal Authority: Monthly Rain\_ACP\_Vertical.xlsx.  
379 <https://doi.org/10.25573/data.10304306.v8>

380 Paton, S. 2025. *2024 Meteorological and Hydrological Summary for Barro Colorado Island*.  
381 Smithsonian Tropical Research Institute.  
382 [https://smithsonian.figshare.com/articles/dataset/Yearly\\_Reports\\_Barro\\_Colorado\\_Island](https://smithsonian.figshare.com/articles/dataset/Yearly_Reports_Barro_Colorado_Island/11799111)  
383 [/11799111](https://smithsonian.figshare.com/articles/dataset/Yearly_Reports_Barro_Colorado_Island/11799111)

384 Paton, S., and R. F. Stallard. in preparation. The climate of Barro Colorado Island. In *The First*  
385 *100 Years of Research on Barro Colorado Island: The Physical Basis*, ed. R. F. Stallard.  
386 Washington, DC: Smithsonian Institution Scholarly Press.

387 Pebesma, E. J., and R. S. Bivand. 2005. Classes and methods for spatial data in R. *R News*, 5: 9-  
388 13

389 Pollock, M. D., G. O'Donnell, P. Quinn, M. Dutton, A. Black, M. E. Wilkinson, M. Colli, M.  
390 Stagnaro, L. G. Lanza, E. Lewis, C. G. Kilsby, and P. E. O'Connell. 2018. Quantifying  
391 and Mitigating Wind-Induced Undercatch in Rainfall Measurements. *Water Resources*  
392 *Research*, 54: 3863-3875. [https://doi.org/https://doi.org/10.1029/2017WR022421](https://doi.org/10.1029/2017WR022421)

393 Retalis, A., Tymvios, F., Katsanos, D., & Michaelides, S. (2017). Downscaling CHIRPS  
394 precipitation data: an artificial neural network modelling approach. *International Journal*  
395 *of Remote Sensing*, 38(13), 3943–3959. <https://doi.org/10.1080/01431161.2017.1312031>

396 Schwalb-Willmann, J. (2024). *basemaps: Accessing Spatial Basemaps in R* (Version R package  
397 version 0.0.7). <https://CRAN.R-project.org/package=basemaps>

398 Team, R. C. 2022. *R: A language and environment for statistical computing*. R Foundation for  
399 Statistical Computing (Vienna, Austria). <https://www.R-project.org/>

- 400 Tennekes, M. 2018. tmap: Thematic Maps in R.: *Journal of Statistical Software*, 84: 1-39.  
401 <https://doi.org/10.18637/jss.v084.i06>
- 402 Trenberth, K. E., D. P. Stepaniak, J. W. Hurrell, and M. Fiorino. 2001. Quality of Reanalyses in  
403 the Tropics. *Journal of Climate*, 14: 1499-1510. [https://doi.org/10.1175/1520-  
404 0442\(2001\)014<1499:QORITT>2.0.CO;2](https://doi.org/10.1175/1520-0442(2001)014<1499:QORITT>2.0.CO;2)
- 405 Vasquez, Vicente. 2024. VasquezVicente/ClimatePanama: precipPanama0.1. Zenodo.  
406 <https://doi.org/10.5281/zenodo.14041384>
- 407 Wright, S. J., and H. C. Muller-Landau. 2024. A Century of Plant and Ecosystem Research at  
408 Barro Colorado. In *The First 100 Years of Research on Barro Colorado: Plant and  
409 Ecosystem Science*, ed. H. C. Muller-Landau and S. J. Wright, pp. 3-16. Washington,  
410 D.C.: Smithsonian Institution Scholarly Press. <https://doi.org/10.5479/si.27180384>

411 Table 1. Key characteristics of the gridded climate products analyzed here. See Table S1 for the larger set of datasets considered for analysis.

Name	Forcing datasets	Resolution, degrees (km)	Time period	Native format	Citation
CHELSA 1.2	Reanalysis dataset: ERA interim	0.0083333 (~1 km)	1979-2013	Climatology, monthly timeseries	Karger et al., 2018
CHELSA 2.1	Reanalysis dataset: ERA5	0.0083333 (~1 km)	1981-2010	Climatology, monthly timeseries	Karger et al., 2018
CHELSA EarthEnv	Reanalysis dataset: ERA5	0.0083333 (~1 km)	2003-2016	Daily timeseries	Karger et al., 2021b
CHELSA W5E5	Reanalysis dataset: WFDE5	0.0083333 (~1 km)	1979-2016	Daily timeseries	Karger et al., 2021a
CHIRPS v2.0	Satellite products: TMPA. Observational dataset: GTS and GHCN.	0.05 (~5.5 km)	1981-2022	Monthly timeseries	Funk et al., 2015b
CHPclim v.1.0	Observational dataset: GHCN & FAO. Assisted with satellites	0.05 (~5.5 km)	1980-2009*	Climatologies	Funk et al., 2015a
TerraClimate	Spatially interpolated dataset: WorldClim v2.0. Reanalysis dataset: JRA-55	0.04166667 (~5 km)	1981-2010 1970-2016†	Climatology, monthly timeseries	Abatzoglou et al., 2018
WorldClim v2.1 (Spatially interpolated dataset)	Observational dataset: WMO & FAO	0.0083333 (~1 km)	1970-2000	Climatologies	Fick and Hijmans, 2017
PBCOR CHELSA 1.2	ERA interim & USGS, GRDC, etc.	0.0083333 <sup>§</sup> (~1 km)	1979-2013	Climatologies	Karger et al., 2018; Beck et al., 2020
PBCOR CHPclim	GHCN & FAO & USGS, GRDC, etc.	0.05 (~5.5 km)	1980-2009*	Climatologies	Funk et al., 2015; Beck et al., 2020
PBCOR WorldClim 2.1	WMO & FAO & USGS, GRDC, etc.	0.0083333 <sup>§</sup> (~1 km)	1970-2000	Climatologies	(Fick and Hijmans, 2017; Beck et al., 2020)

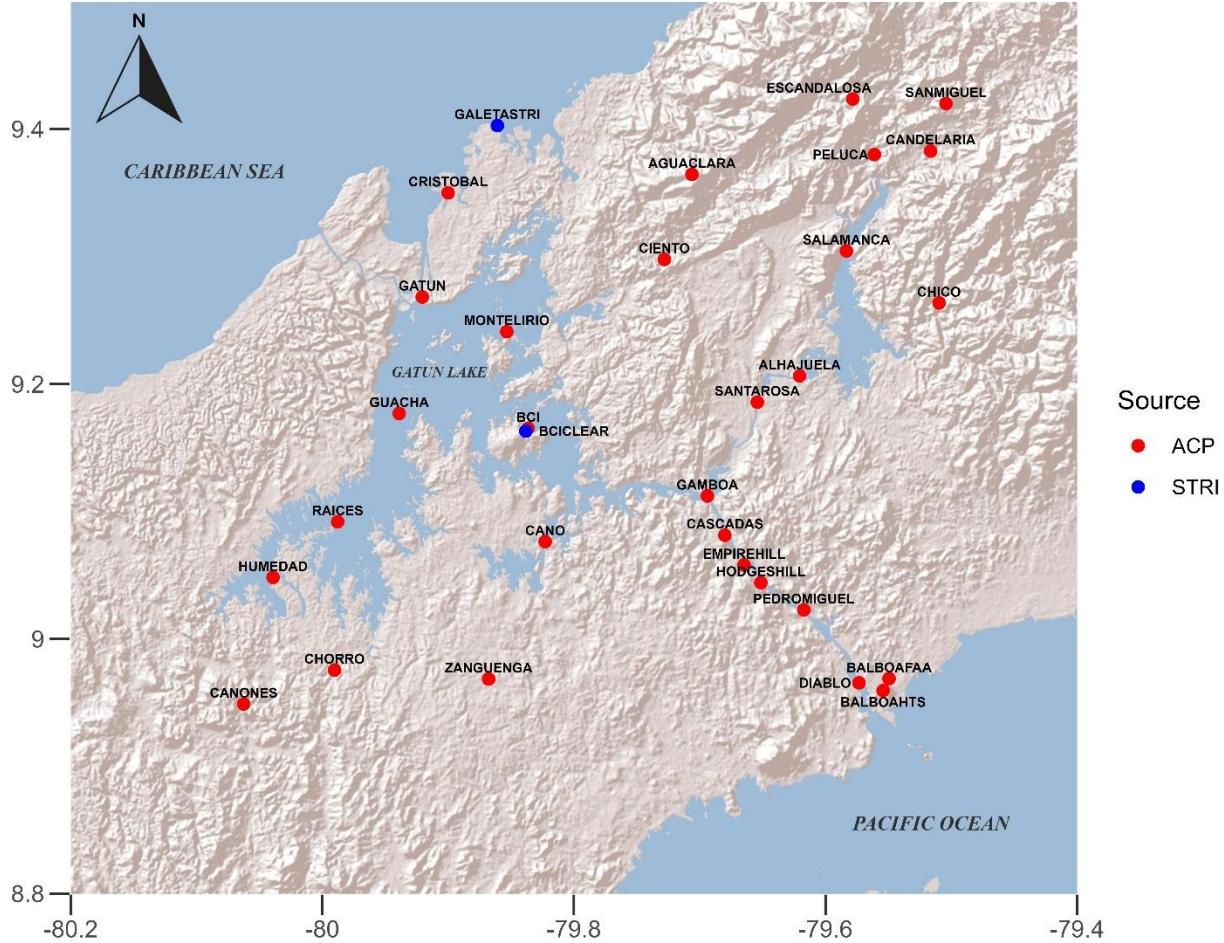
412 \*Adjusted to 1980-2009, although FAO does not provide temporal extent for its climatology

413 †Temporal extent of the complete timeseries extends from 1958 to 2023.

414 <sup>§</sup> PBCOR (Precipitation Bias Correction) versions of products are computed by multiplying the original product by the PBCOR factors. The native  
415 resolution of the PBCOR bias correction factors is 0.05 degrees; these are resampled to the resolution of the original datasets to produce the  
416 bias corrected datasets.

417 Table 2. Summary statistics for the performance of different gridded climate products in relation to the in-situ rain gauge observations  
418 in central Panama. Performance in relation to spatial variation is based on analysis of gap-filled data for 31 stations each having 30 or  
419 more complete years of data during 1970-2016. Performance in reproducing seasonal variation among averages for calendar months  
420 and interannual variation in total annual precipitation is based on nine ground stations with data for 1979-2016 (without gap-filling).  
421 Pearson r is the Pearson correlation coefficient, RMSE is root mean squared error, MAE is mean absolute error, and Bias is the mean  
422 error (see methods). Bold highlights the best performance within each column. Some gridded climate products lacked multiannual  
423 time series and could not be included in the evaluation of interannual variation, indicated here by “NA”.

Gridded Climate Product	Spatial variation in total annual precipitation (31 stations)				Spatial variation in January-to-April precipitation (32 stations)				Seasonal variation (9 stations)		Interannual variation (9 stations)	
	Pearson r	RMS E	MAE	Bias (mm)	Pearson r	RMS E	MAE	Bias (mm)	Pearson r	RMSE	Pearson r	RMSE
CHELSA 1.2	0.82	310	250	53	0.63	107	63	-35	0.97	31	0.31	836
CHELSA 2.1	0.87	475	438	390	0.61	105	69	-6	0.97	42	0.57	608
CHELSA EarthEnv	0.85	318	258	68	0.66	91	61	<b>4</b>	0.94	24	0.59	625
CHELSA-W5E5v1.0	0.36	497	401	<b>-19</b>	0.15	125	83	-10	0.97	42	0.69	657
CHIRPS v2.0	<b>0.88</b>	<b>273</b>	<b>222</b>	92	0.82	<b>81</b>	<b>49</b>	-22	<b>0.98</b>	<b>23</b>	<b>0.74</b>	<b>463</b>
CHPclim v1.0	0.86	371	326	245	<b>0.86</b>	91	57	-46	0.96	29	NA	NA
TerraClimate	0.78	412	346	-50	0.84	112	74	-64	0.93	33	0.27	648
WorldClim 2.1	0.65	402	330	-24	0.47	121	84	-52	0.95	34	NA	NA
PBCOR CHELSA 1.2	0.75	377	306	107	0.60	108	66	-32	0.97	28	NA	NA
PBCOR CHPclim	0.77	547	463	413	0.81	89	54	-32	0.96	36	NA	NA
PBCOR WorldClim 2.1	0.56	423	337	-21	0.32	131	93	-57	0.96	36	NA	NA



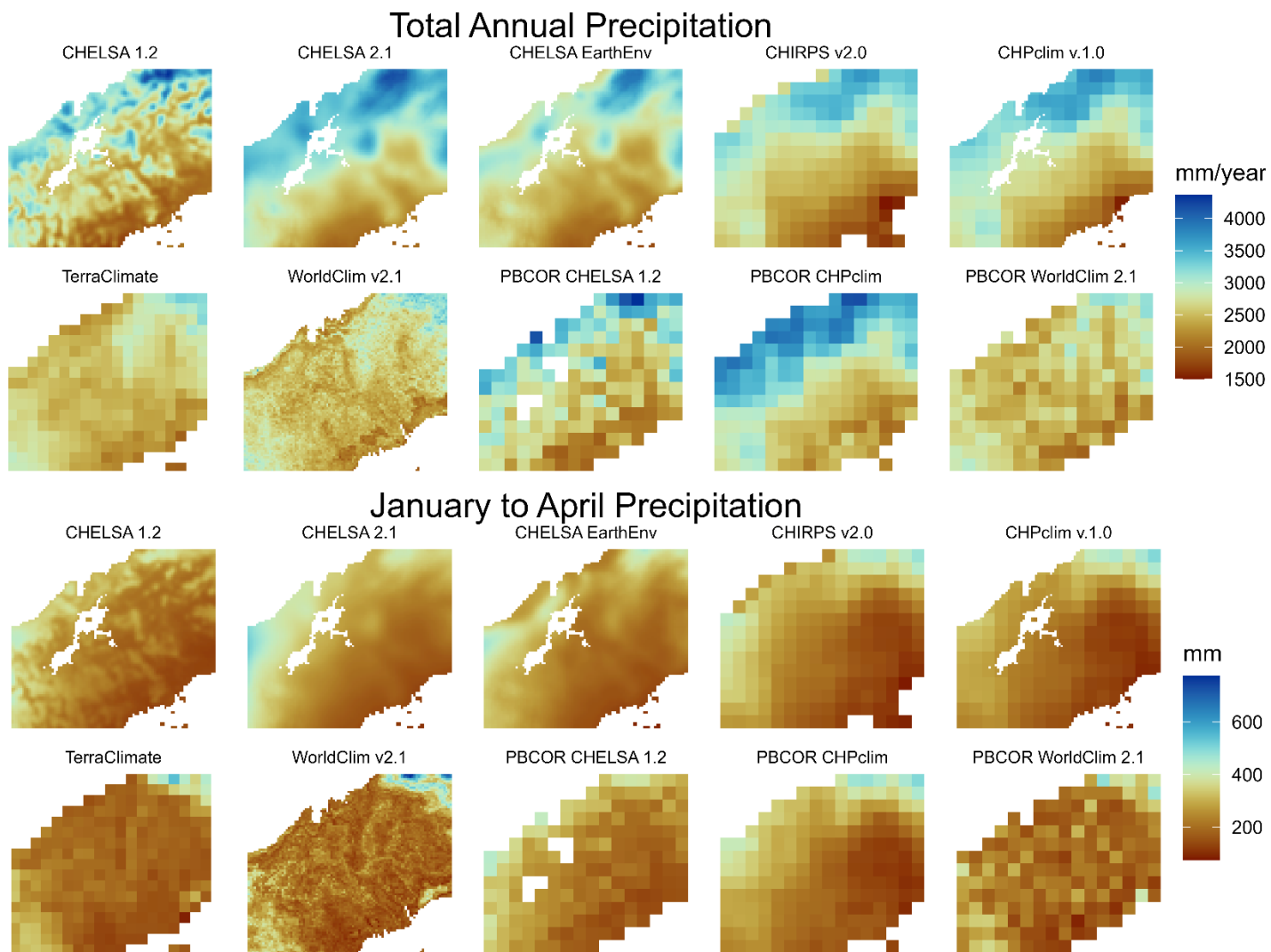
425

426

427 Figure 1. Topographic map of the focal region, indicating the location of in-situ measurement sites used in this analysis including ACP stations

428 (red) and STRI stations (blue).

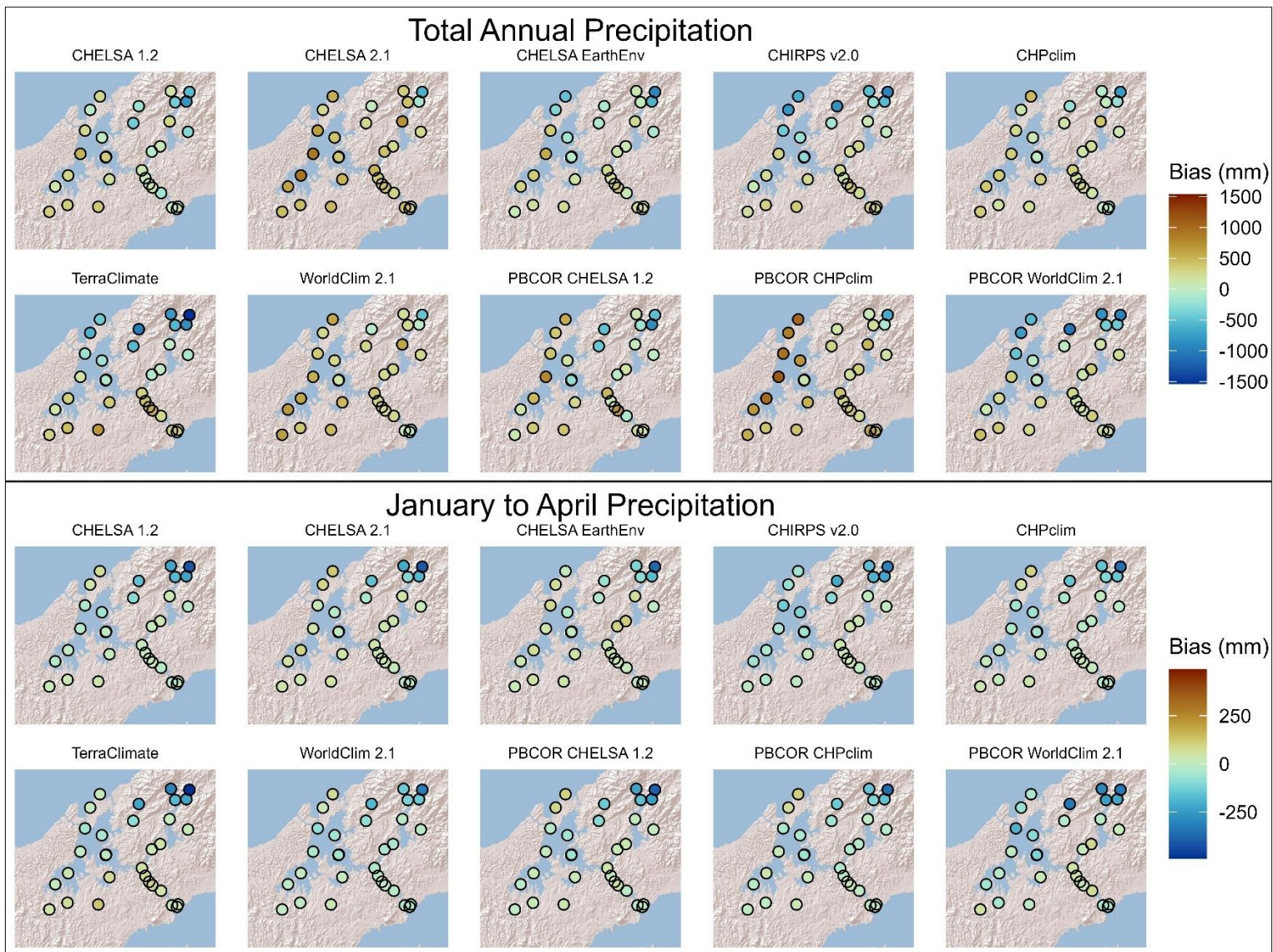
429



430

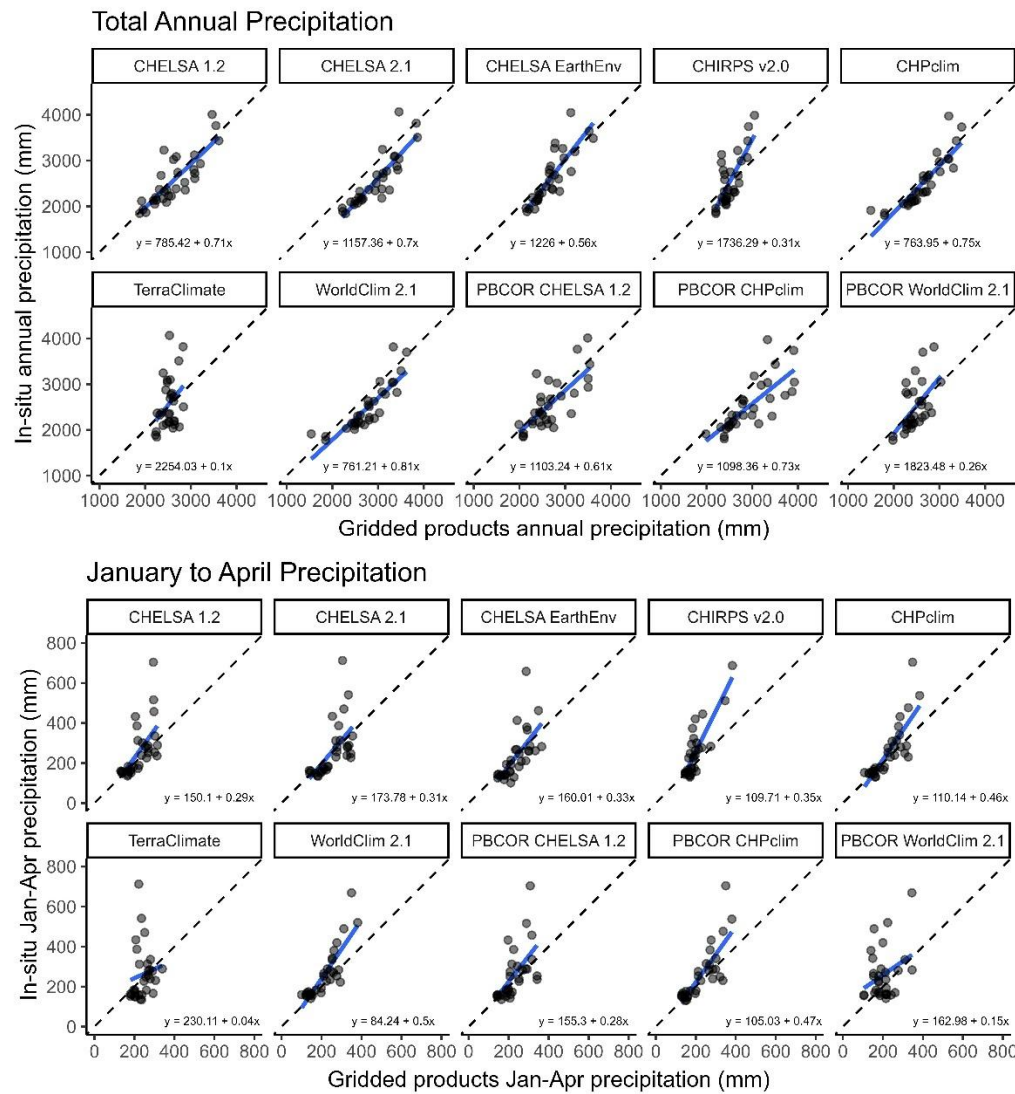
431

432 Figure 2. Spatial patterns in total annual precipitation (top) and January to April precipitation (bottom) for each gridded climate product. Note  
 433 that the temporal range and the spatial resolution vary among datasets (Table 1).



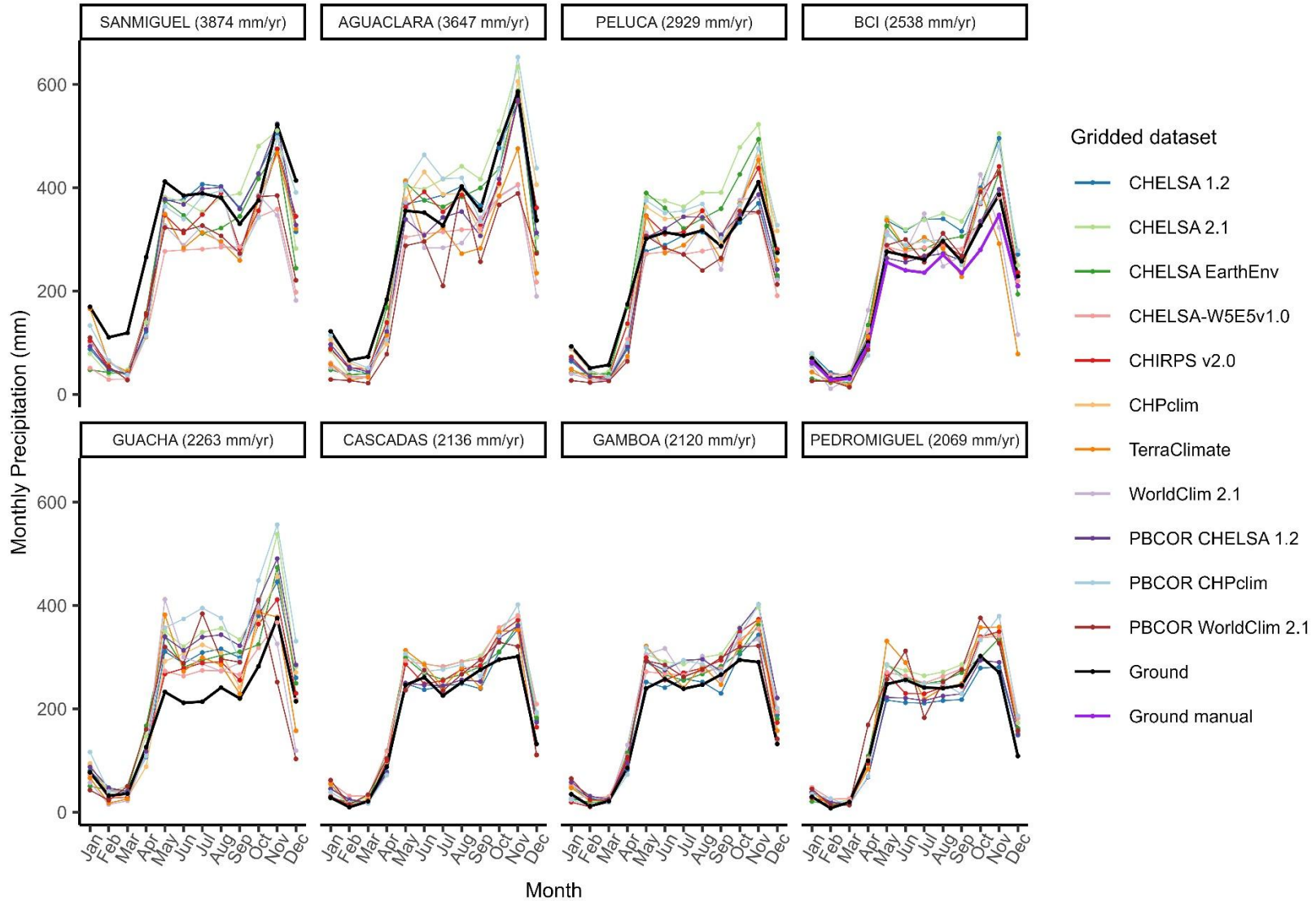
434

435 Figure 3. Spatial patterns of bias (in the gridded climate products in relation to in-situ measurements for total annual precipitation (top) and  
 436 January-April precipitation (bottom).



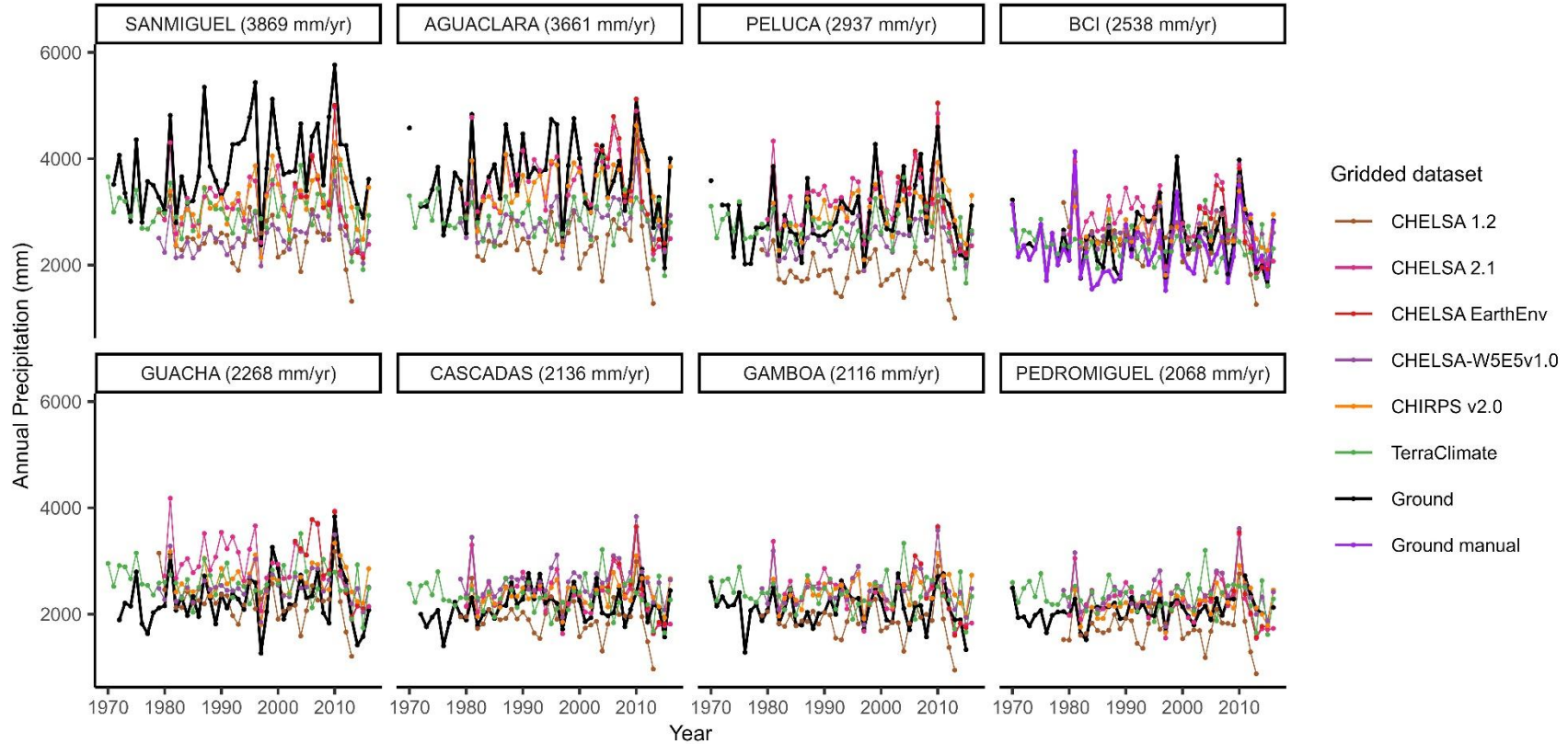
437

438 Figure 4. Comparison of the performance of different gridded climate products in predicting spatial variation in observed precipitation among  
 439 ground datasets in central Panama, for total annual precipitation (top) and January to April precipitation (bottom). Points show individual  
 440 ground stations, black dashed lines show 1:1 lines, and blue lines show type 1 regressions.



441

442 Figure 5. Seasonal patterns in the gridded climate products and in the in-situ observations for nine sites (note that BCI and BCICLEAR are in the  
 443 same grid cell and are graphed as “Ground” and “Ground manual”, respectively). Sites are ordered from highest to lowest rainfall.



444

445 Figure 6. Interannual variability in precipitation in the gridded climate products and in the in-situ observations for nine sites (note that BCI and  
 446 BCICLEAR are in the same grid cell and are graphed as “Ground” and “Ground manual”, respectively). Sites are ordered from highest to lowest  
 447 rainfall.

448

449

450